



ELSEVIER

Physica A 260 (1998) 244–254

202  
**PHYSICA A**

# Isomorphism linking smooth particles and embedded atoms

Wm.G. Hoover\*

*Department of Applied Science, University of California at Davis, Livermore, and Lawrence Livermore National Laboratory, Livermore, CA 94551-7808, USA*

Received 11 June 1998

---

## Abstract

Macroscopic continuum simulations can be based on an unstructured moving spatial grid made up of “smooth particles”. The smooth particles’ equations of motion include interpolated values of the macroscopic stress gradient at each particle’s position. Microscopic solid-state simulations can be based on the motion of “embedded atoms”, with equations of motion based on a physical idea – embedding atoms in the local electronic density. The embedded atoms then move according to Newtonian equations of motion, based on electronic density gradients at each particle position. I show here that these two descriptions, macroscopic smooth particles and microscopic embedded atoms, can give identical particle trajectories. This demonstration facilitates the understanding of macroscopic models for surface tension and also suggests that certain macroscopic continuum approaches to smooth particle applied mechanics could have useful analogs in microscopic molecular dynamics. © 1998 Elsevier Science B.V. All rights reserved.

*PACS:* 02.60; 05.20; 68.10.C; 68.10.M

*Keywords:* Surface tension; Smooth particles; Simulation

---

## 1. Smooth particle applied mechanics

It is appealing to solve continuum problems with a particle method. This is because the ordinary differential equations for particle motion are (i) relatively easy to solve, and (ii) free of the instabilities that plague grid-based methods. Smooth-particle methods are based on two ideas: (i) continuum properties – density, velocity, energy, pressure, and heat flux, for instance – are to be interpolated in space on a discrete irregular particle grid; (ii) the grid particles exchange energy and momentum according to the continuum constitutive relations, where local divergences of the pressure tensor and heat flux vector are evaluated at each particle’s location.

---

\* E-mail: hoover@bonampak.llnl.gov.

In 1977 Monaghan and Lucy independently discovered practical schemes for interpolating continuum properties on a moving grid, and for exchanging momentum and energy among particles [1,2]. The particle locations defined the moving grid, and simultaneously represented the underlying continuum. The spatial influence of each moving particle was described by a normalized short-ranged weight function  $w(r)$ . Useful weight functions need to have at least two continuous derivatives so as to represent solutions of diffusive continuum equations, which incorporate two space derivatives. The simplest of the many examples of such weight functions are Monaghan's and Lucy's, here normalized for two space dimensions:

$$w_{\text{Monaghan}}(r < h/2) \equiv (40/7\pi h^2)[1 - 6(r/h)^2 + 6(r/h)^3],$$

$$w_{\text{Monaghan}}(h/2 < r < h) \equiv (80/7\pi h^2)[1 - (r/h)]^3,$$

$$w_{\text{Lucy}}(r < h) \equiv (5/\pi h^2)[1 + 3(r/h)][1 - (r/h)]^3,$$

$$\int_0^h 2\pi r w(r) dr \equiv 1.$$

At any point in space,  $r$ , local values of the mass, momentum, and energy densities are calculated by summing up the contributions of nearby particles. The local mass density  $\rho_r$ , for instance, is a superposition of contributions from every particle lying within the range  $h$  of the point in question. The mass density at the location of particle  $i$  follows from a special case of the same definition:

$$\rho_r = m \sum_j w_{rj}; \rho_i = m \sum_j w(r_{ij}) = m \sum_j w_{ij}.$$

In such smooth-particle pair sums a typical smooth particle interacts with perhaps 40 of its neighbors. The very smooth character of  $w$ , with  $\nabla w$  and  $\nabla \nabla w$  continuous, guarantees the resulting continuity of both first and second spatial derivatives, such as  $\nabla \rho$ ,  $\nabla^2 T$ , and  $\nabla \cdot P$ .

The smooth-particle form of the continuum equation of motion, in the "Lagrangian" form, following the motion,  $\rho \ddot{r} = -\nabla \cdot P$ , likewise illustrates the simplicity of the gradient operation using smooth particles. The divergence of the pressure tensor, evaluated at the location of particle  $i$ , for instance, becomes a sum of individual particle pressure tensors multiplied by weight-function gradients for all particles within range of particle  $i$ :

$$\ddot{r}_i = -m \sum_j [(P/\rho^2)_i + (P/\rho^2)_j] \cdot \nabla_i w_{ij}.$$

For a fluid isentrope, the pressure in the inviscid smooth-particle equation of motion is hydrostatic, and can therefore be viewed as the derivative of a density-dependent specific energy  $e(v)$ :

$$P = -de/dv = +\rho^2 de/d\rho \rightarrow \ddot{r}_i = m \sum_j [-(de/d\rho)_i - (de/d\rho)_j] \nabla_i w_{ij}.$$

This approach to solving problems in continuum mechanics has a 20-year history of applications to a wide range of flows, as well as to complex deformations in solid mechanics. For references to applications, see recent reviews of the method [1,3,4].

## 2. Molecular dynamics with embedded atoms

Because measured surface and vacancy energies for metals are incompatible with those calculated using simple pair potentials, Daw and Baskes [5] developed a many-body “embedded-atom” potential for use in metallic molecular dynamics simulations. Metal atoms, or nuclei, were viewed as being embedded within a collective electronic density. This density could be calculated by superposing Hartree–Fock wavefunctions or, more simply, by combining weights from nearby atoms,  $\rho_i = m \sum_j w_{ij}$ , where we arbitrarily include the mass  $m$  in this definition to emphasize and enhance the analogy with the smooth-particle models. The weight functions used in the embedded-atom calculations [6,7], for example  $w(r < h) \propto [1 - (r/h)^2]^2$ , were quite similar to the weight functions used in smooth-particle simulations. Note that this embedded-atom example weight function is positive, with compact support. This example has only a single continuous derivative, so that the corresponding simulations are more noisy than their smooth-particle relatives.

The embedded-atom equation of motion, based on the gradient of a potential depending upon all the local particle densities,  $E_{\text{Total}}(r^N) \equiv \sum_i E(\rho_i)$ , is,

$$\begin{aligned} m\ddot{r}_i &= -\nabla_i E_{\text{Total}} = -\sum_j \nabla_i E(\rho_j) \\ &= -m \sum_j [(dE/d\rho)_i + (dE/d\rho)_j] \nabla_i w_{ij} \\ &= -m^2 \sum_j [(de/d\rho)_i + (de/d\rho)_j] \nabla_i w_{ij}. \end{aligned}$$

This motion equation is identical to the smooth-particle form derived in the previous section. Though we had pointed out a resemblance between smooth particles and embedded atoms earlier [3], I first noticed that the corresponding equations of motion are identical while studying the vibrating drop problem described in the next section. We had used exactly the same motion equations previously, to simulate the plastic flow of metals [6,7].

Even when the motion equations for smooth particles and embedded atoms are isomorphic, the two approaches give slightly different expressions for the pressure. The smooth-particle pressure is simply a function of the local density and energy. The embedded-atom pressure tensor has additional contributions from the particle velocities. The embedded-atom form follows from the virial theorem:

$$PV = \sum_i (pp/m) + (rF)_i; \quad F_i = -\nabla_i [\Phi_M + \Phi_P],$$

where the many-body potential  $\Phi_M$  typically has a smooth-particle form, while the “pair” potential  $\Phi_P$  usually does not. In the following section I consider an example in which both parts of the embedded-atom potential have smooth-particle forms.

### 3. Surface tension for drops and for metals

Lord Rayleigh worked out the fundamental theory for the motion of fluid drops governed by surface tension [8]. He showed that the additional pressure within an elliptical drop, as well as its lowest-frequency vibrational mode, could both be expressed in terms of the surface tension  $\sigma$ , the drop radius  $R$ , and the (two-dimensional) mass density  $\rho$ :

$$\Delta P = P_{\text{in}} - P_{\text{out}} = \sigma/R; \quad \omega^2 = 6\sigma/\rho R^3.$$

The first relation results from equating the extra work done by an expanding drop,  $2\pi R dR \Delta P$  to an additional stored surface free energy,  $2\pi\sigma dR$ . The vibrational frequency follows easily by equating the mean kinetic energy to the mean increase in potential energy during the lowest-frequency constant-volume vibration, which has the simple form:

$$x(t) = x(0)[1 + \delta \cos(\omega t)]; \quad y(t) = y(0)[1 - \delta \cos(\omega t)].$$

Some attempts to verify the two relations, for smoothed particles, were based on supplementing the pressure forces with an additional vector “surface force” on each particle, proportional to a neighborhood sum of either  $\nabla w$  or  $r_w$ . Such sums vanish, approximately, in the bulk fluid, but give a substantial nonzero resultant near the surface [3]. This work is summarized in the unpublished theses of Clifford Stein (University of California at Davis, 1998) and Severin Nugent (University of Vienna, in preparation). Though several other investigations of surface tension have been carried out with smooth-particle applied mechanics [9], none has been directed toward a comparison with fundamental atomistic simulations or with confirming Rayleigh’s relations.

When the calculations in the Stein and Nugent theses did not seem to confirm Rayleigh’s relations I set out to make a detailed comparison of them with molecular dynamics simulations, in which surface tension arises automatically, due to the imbalance of forces near the surface. The molecular simulations proceeded by allowing a drop, initially equilibrated in an elliptical enclosure of the proper size, to vibrate freely. Analogous smooth-particle simulations produced very similar results, but without the need for any artificial surface forces of the type considered in Ref. [3] or [9].

It soon became apparent, based on the analyses just given in the two preceding sections, that smooth-particle simulations already contain an artificial surface tension, of order  $\rho e h$ , linear in the range of the weight function and typically larger than the actual surface tension. This larger numerical surface tension can be determined, for instance, by using Rayleigh’s relations to analyze the undamped vibrations of an oscillating drop. It can be estimated by integrating the missing contributions to the binding energy that

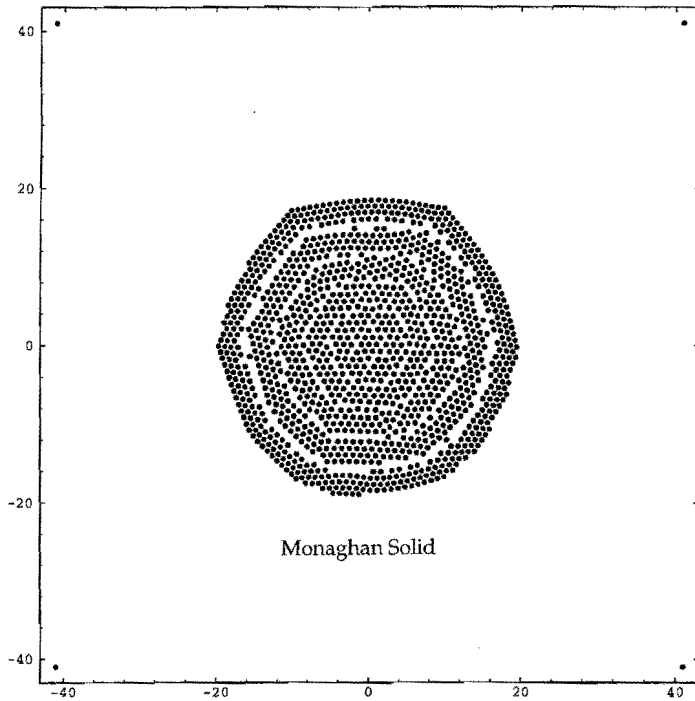
occur near a surface, by assuming a suitable density profile. Unless a much-larger additional surface tension force is imposed, with a range and magnitude somewhat exceeding  $h$ , the artificial numerical surface tension will determine the energy, stress, and morphology at the surface.

Previous analyses have characterized similar size-dependent effects of the smooth particle approach [3,10,11]. These effects are analogs of the finite-difference truncation errors incurred with regular integration grids. These investigations of size dependence have shown that inviscid, insulating fluids, when simulated using smooth particles, exhibit artificial viscosity, artificial heat conductivity, artificial shear moduli and yield strengths, all due to the particulate nature of the approximation, which introduces a graininess, of order  $h$ , into the “continuum”. The present work carries this analogy farther, by pointing out the parallel between macroscopic smooth-particle simulations and a well-known microscopic model for the simulation of atomistic dynamics.

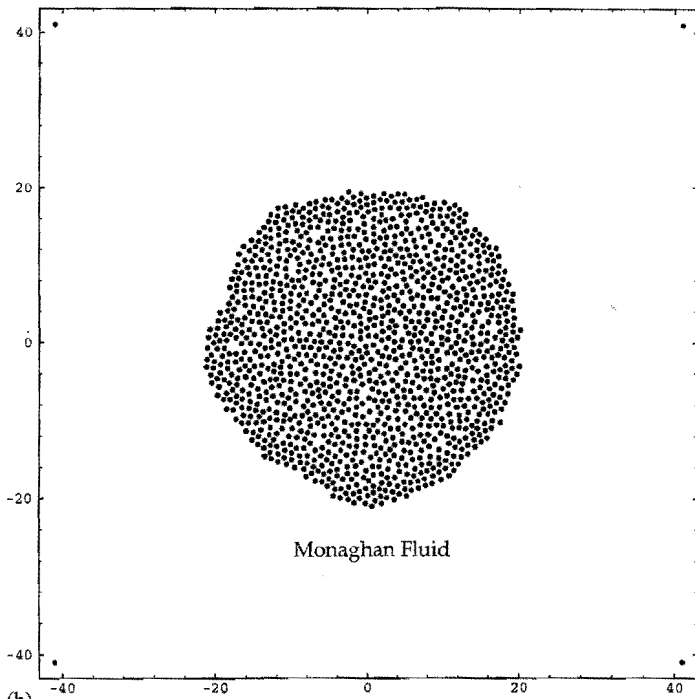
The many-body embedded-atom potential induces an interesting lamellar structure near surfaces, with a characteristic length of order  $h$ , the range of the weighting function. Representative structures, for two different types of weighting functions, are shown as Figs. 1 and 2. These simulations all used a many-body potential  $\Phi_M = \sum_i (\rho_i - 1)^2 / 2$ , where the density was evaluated with a weight function of range  $h$  as well as a “pair potential”,  $\Phi_P = \varepsilon \sum_i \rho_i$ , calculated with a weight function of range unity. A wide variety of weighting functions, ranges, temperatures, initial conditions, and choice of the mixing parameter  $\varepsilon$  was investigated. The structures shown in the Figures are typical of the static solid low-temperature structure and the fluid-drop structure bound by the wholly artificial numerical surface tension of order  $h$ .

Representative energy data are given in Table 1. They show a good straight-line relationship linking the energy per particle to the surface-to-volume ratio,  $\propto \sqrt{1/N}$ . This gives the value  $\sigma = 0.075$ . Separating the potential energy into its pair and many-body components, it is apparent that nearly ninety percent of the surface energy is due to the long-range collective embedded-atom potential contributions. Though the fluid data are much less precise, due to fluctuations, the plots suggest that the same apparent solid surface tension, about 0.075 in reduced units, is also a good estimate for the fluid phase. The bulk equation of state for this embedded-atom model is insensitive to the number of particles used. At a temperature of 0.01 and specific volumes  $\{1.0, 1.025, 1.05, 1.075\}$  the specific energies  $\{0.0155, 0.0155, 0.0156, 0.0167\}$  and compressibility factors  $\{PV\} = \{0.125, 0.0705, 0.016, -0.029\}$  show that a linear stress-strain relation is a good approximation throughout the density range covered by the simulations.

To check that the artificial numerical surface energy, obtained from the data in Table 1, obeys Rayleigh’s relations, isothermal drops were first equilibrated, in elliptical enclosures with a width-to-height ratio  $1.1^2$ , and were then allowed to move freely. The pressures in the interior of these drops were determined by using the virial theorem expression given in the last section, averaged over those particles closest to the center of mass of the drop. Pressure averages, computed with a weight function spanning about one hundred particles, were consistent with Rayleigh’s estimate,  $\sigma/R$ .



(a)



(b)

Fig. 1. 1261-particle simulations using Monaghan's "B-spline" weighting function. The simulation (a) is the stable static structure reached by incorporating damping in the equations of motion where  $\varepsilon = 1/8$  and  $h = 5$ . The structure (b) is a typical fluid-drop snapshot, at a temperature of 0.01, with  $\varepsilon = 1$  and  $h = 5$ .

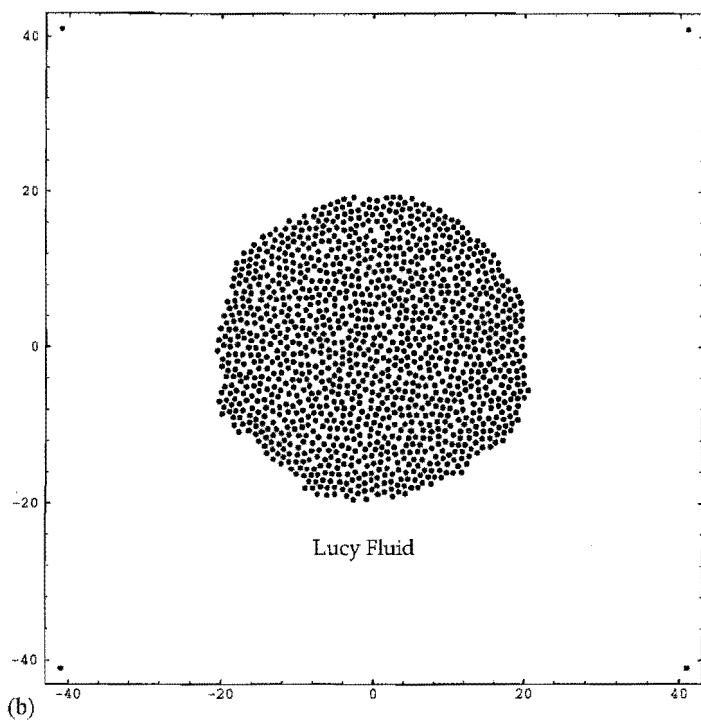
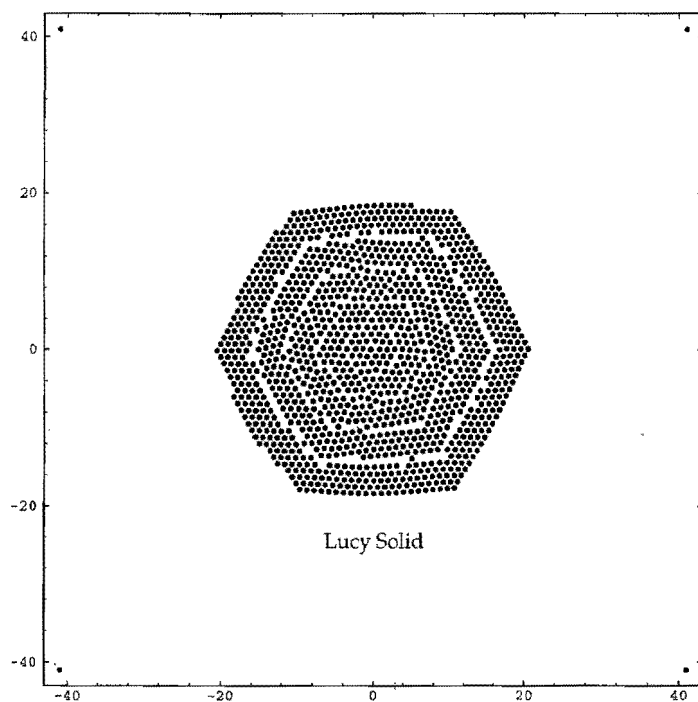


Fig. 2. 1261-particle simulations using Lucy's weighting function, as described in the text. The simulation (a) is the stable static structure reached by incorporating damping in the equations of motion where  $\varepsilon = 1$  and  $h = 5$ . The structure (b) is a typical fluid-drop snapshot, at a temperature of 0.01, with  $\varepsilon = 1$  and  $h = 5$ .

Table 1

Pair and many-body energies per particle for Lucy-weighted smooth-particle embedded-atom simulations with  $\Phi = \sum \phi_{ij} + \sum (\rho_i - 1)^2/2$ , where the pair function  $\phi = w_{\text{Lucy}}$  has unit range and the density  $\rho_i$  was computed with a Lucy function with range 5. The particle mass has been chosen equal to unity. All calculations began with a regular hexagonal structure. Both fluid ( $T = 0.01$ ) and solid ( $T = 0.00$ ) results are included. For each the pair potential energy is given first, followed by the many-body energy, with both energies averaged over the entire simulation. These entries are followed by the total potential energy at the conclusion of each run. All of the simulations were carried out for a time of 1000 with a fourth-order Runge Kutta integrator. The “solid” simulations included a viscous damping force,  $-0.1v$ , and converged to stable energy minima.

$N$		$(\Phi/N)_{\text{fluid}}$		$(\Phi/N)_{\text{solid}}$		
217	0.0063	0.0184	0.0238	0.0015	0.0116	0.0127
331	0.0058	0.0152	0.0212	0.0011	0.0092	0.0099
469	0.0056	0.0130	0.0183	0.0009	0.0076	0.0082
631	0.0053	0.0115	0.0171	0.0009	0.0064	0.0070
817	0.0052	0.0104	0.0156	0.0007	0.0056	0.0060
1027	0.0050	0.0097	0.0146	0.0006	0.0050	0.0054
1261	0.0049	0.0089	0.0136	0.0006	0.0044	0.0047
1519	0.0048	0.0085	0.0129	0.0006	0.0040	0.0043
1801	0.0047	0.0080	0.0126	0.0006	0.0036	0.0039
2107	0.0046	0.0077	0.0124	0.0005	0.0034	0.0037

The phase of the surface-tension-induced vibrations was estimated by plotting the time development of the diagonal elements of the moment of inertia tensor, as shown in Fig. 3. The plot indicates an oscillation time of order  $\tau = 1400$  for a 2107-particle with a drop radius of 27. The theoretical calculation, using the surface tension from Fig. 1 gives  $\tau = 1260$ . I conclude that the numerical surface tension exhibited by smooth particles (or embedded atoms) follows the usual principles of mechanics. The magnitude of this property is most easily determined from its effect on vibrations.

The interesting lamellae which form, even in the drops, are readily apparent in these two-dimensional simulations, and are reminiscent of similar structures seen in earlier metal simulations, as well as in the macroscopic simulations shown in Ref. [4] and other smooth-particle papers. At low temperature, the lamellar structure extends quite far from the surface. At higher temperatures, where the structure is definitely fluid, the layering effect is only visible as a shell surrounding an otherwise quite-disordered interior region.

#### 4. Conclusion

The isomorphism linking smooth-particle and embedded-atom simulations shows that the smooth-particle methods possess an artificial surface tension (of order  $\rho eh$ ). The analogy between the macroscopic and microscopic simulations explains the presence of this property, as well as artificial viscosity, conductivity, and shear moduli, on physical grounds. Pictures of macroscopic smooth-particle simulations show the same layered structure, as do also embedded-atom simulations. Evidently these structures are

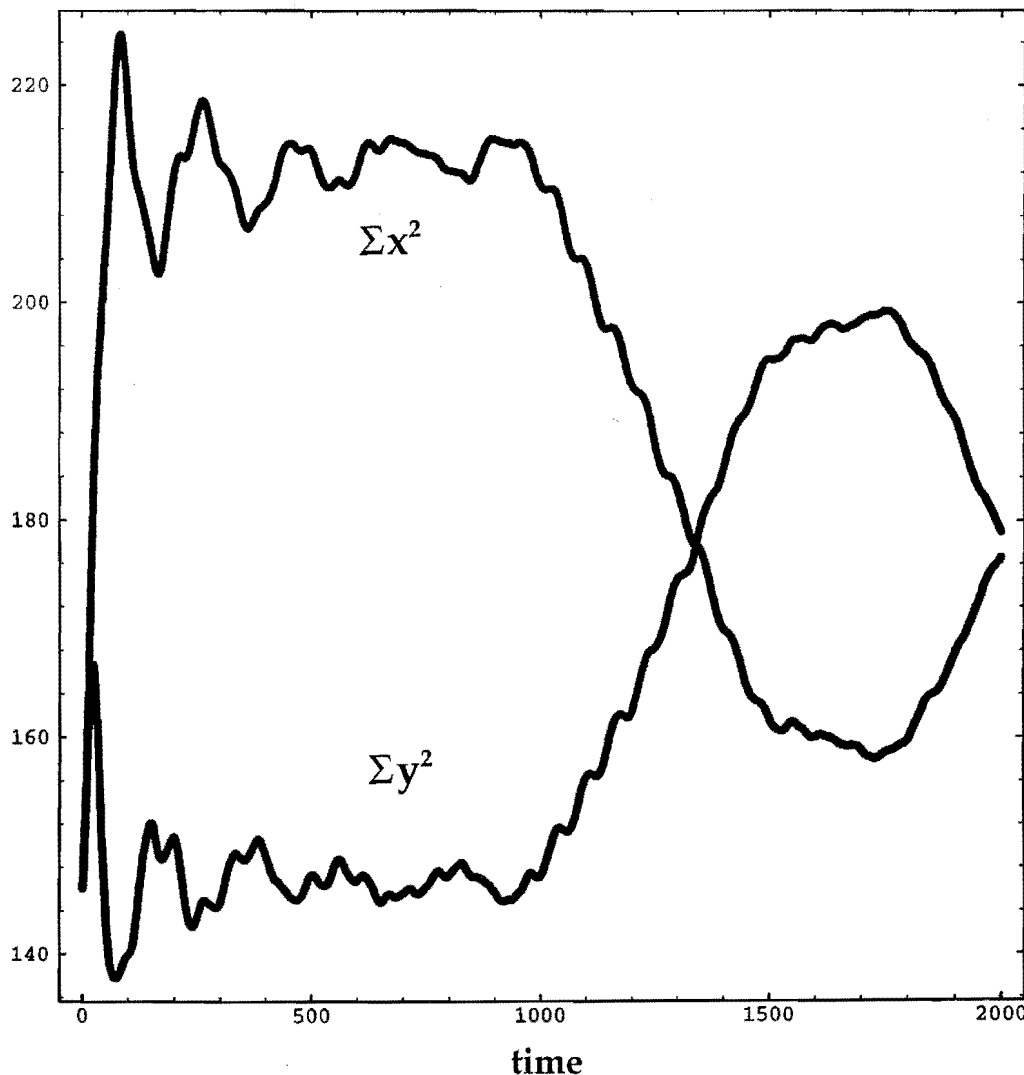


Fig. 3. Time history of the  $\langle x^2 \rangle$  and  $\langle y^2 \rangle$  for an initially elliptic drop of 2107 particles. The elliptical enclosure and the constraint fixing the kinetic energy were both removed at time 1000, after which the drop oscillated, following Newton's equations of motion.

characteristic of the functional dependence of the energy on the coordinates through an intermediate density function.

The finding that embedded-atom simulations can be formulated in terms of smooth-particle algorithms suggests that other versions of the smooth-particle algorithm could be applied to the simulation of metals. It should be noted that the form  $(P/\rho^2)_i + (P/\rho^2)_j$  which appears in the equations of motion for smooth particles can equally well be rendered as  $(P_i + P_j)/(\rho_i \rho_j)$  or, at the expense of momentum conservation, as

$$(\rho^2 \ddot{r})_i = m \sum [P_i - P_j] \cdot \nabla_i w_{ij}.$$

These for  
to solve s  
state and

After r  
evaluatio  
a sum o  
researche  
equations

{ $\rho$

The sim  
differenti

{ $\dot{\rho}$

It turn  
approach  
compute  
by no m  
follows

[ $\rho$

In most  
polytrop  
density  
motion  
waves i

In the  
and sur  
density.  
about t  
each pe  
grow as  
fluid-dr

Ackno

This  
auspice  
Contra  
vanced

These forms, and others, together with the wide variety of algorithms already developed to solve smooth-particle equations [2,4], may well have interesting applications to solid-state and molten-metal physics.

After reading an earlier draft of this manuscript, Jeff Swegle suggested that alternative evaluations of the smooth-particle density, using the continuity equation rather than a sum of weight functions, could reduce the surface effects just discussed. Several researchers have computed particle densities by integrating the corresponding continuity equations over time:

$$\{\rho_i^{\text{int}}(t) \equiv \rho_i^{\text{int}}(0) + \int_0^t \dot{\rho}_i^{\text{int}}(t') dt'\}.$$

The simplest such approach evaluates the set of time derivatives  $\{\dot{\rho}_i^{\text{int}}\}$  by chain-rule differentiation:

$$\{\dot{\rho}_i^{\text{int}} \equiv m \sum (v_i - v_j) \cdot \nabla_i W_{ij}\}.$$

It turns out that the surface properties described here are not eliminated by this approach. For any given set of particle trajectories  $\{r_i(t)\}$  it is evident that the densities computed by summing weights can differ from the continuity-equation particle densities by no more than the set of integration constants  $\{\rho_i^{\text{int}}(0) - \rho_i^{\text{sum}}(0)\}$ . This conclusion follows simply from the identities.

$$[\rho_i^{\text{sum}}(t) - \rho_i^{\text{sum}}(0)] \equiv [\rho_i^{\text{int}}(t) - \rho_i^{\text{int}}(0)].$$

In most problems the detailed trajectories would have to differ. An exception is the polytropic equation of state,  $P \propto \rho^2$ , for which the trajectories are independent of the density definition. This particular polytropic equation of state describes both (i) the motion of a two-dimensional ideal gas of point particles and (ii) the propagation of waves in shallow water.

In the context of the two-dimensional fluid-drop simulations described here the bulk and surface particles have densities  $\{\rho_i^{\text{sum}}\}$  lying within about 20 percent of the mean density. Additional simulations, carried out to follow up Swegle's suggestion, show that about this same range of densities develops using the integral densities  $\{\rho_i^{\text{int}}\}$ , where each particle starts out with an initial density of unity. The integral-density disparities grow as "surface" particles migrate to the "interior" and *vice versa*. Thus, in Rayleigh's fluid-drop problem neither approach eliminates substantial surface effects.

### Acknowledgements

This work was performed at the Lawrence Livermore National Laboratory, under the auspices of the United States Department of Energy through University of California Contract W-7405-Eng-48 and with the support of the Accelerated Strategic and Advanced Scientific Computing Initiatives. I specially thank Brad Holian, Norm Johnson,



the elliptical  
 ich the drop  
  
 s through  
  
 f smooth-  
 hm could  
 $(P/\rho^2)_i +$   
 1 equally  
 ervation,

and Charles Wingate, at Los Alamos, together with Harald Posch, at the University of Vienna, for helpful suggestions and advice. Joe Monaghan kindly provided his own unpublished notes on the incorporation of surface tension into smooth-particle simulations. Clifford Stein and Severin Nugent provided the stimulation necessary to carry out this work. Chuck Leith pointed out to me the applicability of the polytropic equation of state to shallow water waves, as is discussed in Landau and Lifshitz' text on fluid mechanics.

## References

- [1] J.J. Monaghan, *Ann. Rev. Astron. Astrophys.* 30 (1992) 543.
- [2] L. Lucy, *Astron. J.* 82 (1977) 1013.
- [3] W.G. Hoover, T.G. Pierce, C.G. Hoover, J.O. Shugart, C.M. Stein, A.L. Edwards, *Comput. Math. Appl.* 28 (1994) 155.
- [4] L.A. Crotzer, G.A. Dilts, C.E. Knapp, K.D. Morris, R.P. Swift, C.A. Wingate, *Sphinx Manual*, Los Alamos National Laboratory Report LA-13436-M, April, 1998.
- [5] M.S. Daw, M.I. Baskes, *Phys. Rev. B* 29 (1984) 6443.
- [6] B.L. Holian, A.F. Voter, N.J. Wagner, R.J. Ravelo, S.P. Chen, W.G. Hoover, C.G. Hoover, J.E. Hammerberg, T.D. Dontje, *Phys. Rev. A* 43 (1991) 2655.
- [7] W.G. Hoover, A.J. De Groot, C.G. Hoover, *Comput. Phys.* 6 (1992) 155.
- [8] Lord Rayleigh, *Proc. Roy. Soc. (London)* 29 (1879) 71.
- [9] J.U. Brackbill, D.B. Kothe, C. Zemach, *J. Comput. Phys.* 100 (1992) 335; see also W.C. Welton, *J. Comput. Phys.* 139 (1998) 410.
- [10] Wm.G. Hoover, H.A. Posch, *Phys. Rev. E* 54 (1996) 5142.
- [11] Wm.G. Hoover, S. Hess, *Physica A* 231 (1996) 425.



G  
of

## Abstract

We cor  
cients. Th  
to the cor  
mation at  
in the cas  
as our Or

## Keywords

## 1. Intro

The g  
introduc  
depende  
The p

$\delta I$

$\eta_B, \eta_C$   
 $\eta_m = 1$

$\delta I$